

Published in final edited form as:

Science. 2010 September 3; 329(5996): 1175–1180. doi:10.1126/science.1193225.

## Spiroindolones, a new and potent chemotype for the treatment of malaria

Matthias Rottmann<sup>1,2,\*</sup>, Case McNamara<sup>3,\*</sup>, Bryan K. S. Yeung<sup>4,\*</sup>, Marcus C. S. Lee<sup>5</sup>, Bin Zou<sup>4</sup>, Bruce Russell<sup>6</sup>, Patrick Seitz<sup>1,2</sup>, David M. Plouffe<sup>3</sup>, Neekesh V. Dhar<sup>7</sup>, Jocelyn Tan<sup>4</sup>, Steven B. Cohen<sup>3</sup>, Kathryn R. Spencer<sup>7</sup>, Gonzalo E. González-Páez<sup>7</sup>, Suresh B. Lakshminarayana<sup>4</sup>, Anne Goh<sup>4</sup>, Rossarin Suwanarusk<sup>6</sup>, Tim Jegla<sup>7</sup>, Esther K. Schmitt<sup>8</sup>, Hans-Peter Beck<sup>1,2</sup>, Reto Brun<sup>1,2</sup>, Francois Nosten<sup>9,10,11</sup>, Laurent Renia<sup>6</sup>, Veronique Dartois<sup>4</sup>, Thomas H. Keller<sup>4</sup>, David A. Fidock<sup>5,12</sup>, Elizabeth A. Winzeler<sup>3,7,#</sup>, and Thierry T. Diagana<sup>4,#</sup>

<sup>1</sup> Swiss Tropical and Public Health Institute, Parasite Chemotherapy, CH-4002 Basel, Switzerland

<sup>2</sup> University of Basel, CH-4003 Basel, Switzerland <sup>3</sup> Genomics Institute of the Novartis Research Foundation, San Diego, CA 92121, USA <sup>4</sup> Novartis Institute for Tropical Diseases, 138670 Singapore <sup>5</sup> Department of Microbiology and Immunology, Columbia University Medical Center, NY 10032, USA <sup>6</sup> Laboratory of Malaria Immunobiology, Singapore Immunology Network, Agency for Science Technology and Research (A\*STAR), Biopolis, Singapore <sup>7</sup> Department of Cell Biology, The Scripps Research Institute, La Jolla, CA 92037, USA <sup>8</sup> Natural Products Unit, Novartis Pharma AG, CH-4002 Basel, Switzerland <sup>9</sup> Shoklo Malaria Research Unit, Mae Sot, Tak 63110, Thailand <sup>10</sup> Faculty of Tropical Medicine, Mahidol University, Bangkok, Thailand <sup>11</sup> Centre for Tropical Medicine, Nuffield Department of Clinical Medicine, University of Oxford, OX3 7LJ, UK <sup>12</sup> Department of Medicine (Division of Infectious Diseases), Columbia University Medical Center, NY 10032, USA

### Abstract

Recent reports of increased tolerance to artemisinin derivatives—the last widely effective class of antimalarials — bolster the medical need for new treatments. The spiro-tetrahydro- $\beta$ -carboline, or spiroindolones, are a new class of fast-acting and potent schizonticidal drugs displaying low nanomolar potency against *Plasmodium falciparum* and *Plasmodium vivax* clinical isolates. Spiroindolones rapidly diminish protein synthesis in *P. falciparum*, an effect that is ablated in parasites bearing non-synonymous mutations in the gene encoding the P-type cation-transporter ATPase4 (PfATP4). The optimized spiroindolone NITD609 shows an acceptable safety profile and pharmacokinetic properties compatible with once-daily oral dosing; and demonstrates single-dose efficacy in a rodent malaria model. Collectively, these data demonstrate that NITD609 possesses a pharmacological profile suitable for a new drug candidate for the treatment of malaria.

Globally, 3.3 billion people are exposed to malaria, a devastating disease that causes over 800,000 deaths each year and kills more under five-year-olds than any other infectious agent (1). Fifty years ago, malaria had been eliminated from many areas of the world through effective antimalarial drug treatments, vector control interventions and disease prevention

#Corresponding authors (Winzeler@scripps.edu and Thierry.diagana@novartis.com).

\*These authors equally contributed to this work

#### One-sentence summary

We describe the pharmacological profile of a new antimalarial drug candidate—the spiroindolone NITD609—which through a novel mechanism of action rapidly clears a *Plasmodium* infection upon administration of a single oral dose in a malaria mouse model.

(2). However, the global spread of drug resistance resulted, by the 1980s, in a substantial increase in disease incidence and mortality. Today, some encouraging epidemiological data suggest that the introduction of new drugs (notably the artemisinin-based combination therapies or ACTs) may have reversed that trend (3). Derivatives of the endoperoxide artemisinin constitute the only antimalarial drugs that remain effective in all malaria-endemic regions, but recent reports suggest that decades of continuous use as monotherapies might have fostered the emergence of resistance (4–6). This realization has triggered a concerted search for new drugs that could be deployed if artemisinin resistance were to spread.

Many of the therapies currently in development utilize known antimalarial pharmacophores (e.g. aminoquinolines and/or peroxides) chemically modified to overcome the liabilities of their predecessors (7). While these compounds may prove to be important in the treatment of malaria, it would be preferable to discover novel chemotypes with a distinct mechanism of action (8). However, despite significant advances in our understanding of *Plasmodium* genome biology, the identification and validation of new drug targets has proven challenging (9).

To identify novel antimalarial leads, we and others have screened diverse chemical libraries using *Plasmodium* whole-cell proliferation assays with cultured intra-erythrocytic parasites (10–12). From a library of about 12,000 pure natural products and synthetic compounds with structural features found in natural products, our screen identified 275 primary hits with sub-micromolar activity against the most lethal human malarial parasite *P. falciparum*. We discarded those hits whose activity was not reconfirmed against multi-drug resistant parasites and/or that displayed some cytotoxicity against mammalian cells (more than 50% inhibition at 10  $\mu$ M). Pharmacokinetic and physical properties were then determined for the remaining 17 compounds. From this, a synthetic compound related to the spiroazepineindole class, having a favorable pharmacological profile, stood out as an attractive chemical starting point for a medicinal chemistry lead optimization effort. Synthesis and evaluation of about 200 derivatives yielded the optimized spirotetrahydro- $\beta$ -carboline (or spiroindolone) compound NITD609 (Fig. 1A). This compound is synthesized in eight steps including chiral separation of the active enantiomer, and is amenable to large-scale manufacturing. NITD609 has good drug-like attributes (see below) and displays physicochemical properties compatible with conventional tablet formulation.

There is general agreement that a new antimalarial should ideally meet the following criteria: (i) display cidal activity against the parasite blood stages; (ii) be active against drug-resistant parasites, (iii) have no intrinsic safety liabilities (e.g. cytotoxicity, genotoxicity and/or cardiotoxicity), and finally (iv) have pharmacokinetic properties compatible with once-daily oral dosing. The data reported below demonstrate that NITD609 meets all of the criteria for a new antimalarial. We also provide insights into a mechanism of drug resistance involving the P-type cation-transporter ATPase4 (PfATP4).

## Spiroindolones display fast and potent blood-schizonticidal activity against drug-resistant *Plasmodium*

Antimalarial blood-stage activity was evaluated *in vitro* against a panel of culture-adapted *P. falciparum* strains. NITD609 displayed low nanomolar IC<sub>50</sub> values (range 0.5–1.4 nM; Table S1), with no evidence of diminished potency against drug-resistant strains (Table S1). This compound was also tested in *ex vivo* assays with fresh isolates of *P. falciparum* and *P. vivax* (13), collected from malaria patients on the Thai-Burmese border where drug resistance has been widely reported (14,15). NITD609 was found to be as effective as artesunate, with potency in the low nanomolar range (IC<sub>50</sub> values consistently <10 nM).

against all *P. falciparum* (Fig. 1B) and *P. vivax* (Fig. 1C) isolates. NITD609 is also similar to artesunate in its ability to kill both mature trophozoite and immature *P. vivax* ring stages, in contrast to the trophozoite stage-specific activity observed with chloroquine (16). Regardless of their initial developmental stages, NITD609-treated parasites rapidly displayed morphological hallmarks of dying parasites, including pycnotic nuclei and abnormal digestive vacuoles and/or nuclear segmentation. Collectively, our *in vitro* and *ex vivo* data show that spiroindolones are potent against the intra-erythrocytic stages of the major human malarial pathogens *P. falciparum* and *P. vivax*, including a range of drug-resistant strains.

The rapid activity of artemisinin derivatives against all *Plasmodium* asexual erythrocytic stages is a key feature of their excellent therapeutic efficacy (6). To precisely determine which parasite blood stages are most sensitive to the spiroindolones, and to evaluate the time required for these drugs to act, we conducted *in vitro* drug sensitivity assays with synchronized parasites treated at ring, trophozoite and schizont stages for various durations (1, 6, 12 and 24 hours) prior to removal of drug and continuation of culture for 24 hours in the presence of [<sup>3</sup>H]-hypoxanthine. At a high concentration of NITD609 ( $\approx 100 \times \text{IC}_{50}$  value), all stages (rings, trophozoites and schizonts) were similarly sensitive (Fig. S1). However, at low concentrations ( $\approx (1 \text{ or } 10 \times \text{IC}_{50})$  value), schizonts were the most susceptible. These data suggest that the target is present in all asexual blood stages but might be particularly vulnerable in schizonts. With respect to drug action, while clearly significantly faster-acting than the former first-line antifolate agent pyrimethamine, NITD609 did not inhibit parasite growth as quickly as the artemisinin derivative artemether (Fig. S1). Strong inhibition was achieved with artemether treatment at 8 nM for only 6 hours, whereas similar activity was achieved with NITD609 at 1.6 nM for 24 hours.

Although at least 12 hours of continuous drug exposure was required to reduce by 90% the incorporation of [<sup>3</sup>H]-hypoxanthine into parasite DNA (Fig. S1), a [<sup>35</sup>S]-radiolabelled methionine and cysteine ([<sup>35</sup>S]-Met/Cys) incorporation assay revealed that NITD609 effectively blocked protein synthesis in *P. falciparum* parasites within one hour (Fig. 2A). A similar effect was observed with the known protein translation inhibitors anisomycin (an inhibitor of peptidyl transferase) and cycloheximide (an inhibitor of translocation activities during polypeptide elongation). In contrast, the antimalarial drugs artemisinin and mefloquine only showed a nominal decrease in [<sup>35</sup>S]-Met/Cys incorporation within one hour. These data suggest that NITD609 has a mechanism of action different from artemisinin and mefloquine.

## The spiroindolone NITD609 has a large selectivity index and displays an acceptable safety profile

Considering the malaria patient population—mostly young children and pregnant women—and the resource limitations in providing adequate medical supervision of treatment, new antimalarial drug candidates require a very good safety profile. To assess for intrinsic cytotoxic activity, we measured the concentration leading to 50% cell death ( $\text{CC}_{50}$ ) *in vitro* with cell lines of neural, renal, hepatic or monocytic origins. With NITD609, no significant cytotoxicity was observed ( $\text{CC}_{50} > 10 \mu\text{M}$ ; Table S2). Given that NITD609 has an  $\text{IC}_{50}$  of  $\sim 1 \text{ nM}$  against *P. falciparum* (Table S1), the cytotoxicity data establish a selectivity index ( $\text{CC}_{50}/\text{IC}_{50}$ )  $> 10,000$ . Multiple antimalarial drugs have cardiotoxicity liabilities due to hERG channel inhibition, which in extreme cases has resulted in their withdrawal (17,18). hERG binding and patch clamp assays with NITD609 yielded  $\text{IC}_{50}$  values  $> 30 \mu\text{M}$ , consistent with a very low risk of cardiotoxicity (Table S3). Using a miniaturized Ames assay, we also established that NITD609 lacked intrinsic mutagenic activity. Finally, we

observed no significant binding with a panel of human G-protein coupled receptors, enzymes and ion channels (Table S4).

In agreement with these *in vitro* data, male rats tolerated an oral administration of NITD609 daily for 14 days at a dose yielding daily exposure ( $AUC_{0-24h}$ ) values between 29,400 and 56,500 ng\*h/ml. This is equivalent to 10 to 20 times the daily exposure to a dose that reduced parasitemia by 99% in a malaria mouse model ( $ED_{99} = 5.3$  mg/kg; see below). Under these conditions, no adverse events or significant histopathological findings were observed. Overall, these data show that NITD609 has an acceptable safety profile for a new antimalarial drug.

## **The clinical candidate NITD609 shows favorable pharmacokinetic properties and displays single dose cure efficacy in a malaria mouse model**

Having shown that our lead spiroindolone NITD609 fulfills the first three criteria for a new antimalarial drug candidate, we determined its pharmacokinetic properties. Upon oral and intravenous administration in mice and rats, this compound displayed a moderate volume of distribution and a low total systemic clearance (Table S5). Orally administered NITD609 was well absorbed, and displayed a long half-life and excellent bioavailability. Based on our *in vitro* metabolic stability data, this favorable profile is likely to extend to humans, as the predicted metabolic clearance for this compound was low across several species (Table S6). Taken together, these data suggest that NITD609 displays favorable pharmacokinetic properties consistent with once-daily oral dosing. We tested this drug candidate through the oral route in a virulent *P. berghei* malaria mouse model (19,20). The results of these experiments show that NITD609 displays efficacious doses ( $ED_{50/90/99} = 1.2, 2.7, \text{ and } 5.3$  mg/kg) that are lower than those of the reference antimalarial drugs chloroquine, artesunate and mefloquine (Table S7). A single oral dose of NITD609 at 100 mg/kg was found to completely clear *P. berghei* infection in all treated mice, and partial cure (50%) was achieved with a single oral dose at 30 mg/kg (Table 1). Three daily oral doses of 50 mg/kg allowed for complete cure and partial cure (90%) was achieved at 3x30 mg/kg (Table S8). At similar dosing regimens, none of the reference drugs tested could achieve even partial cure in this lethal infection model. To our knowledge, among the drug candidates currently in development, only the new-generation synthetic peroxide compounds (e.g. OZ439) have been reported to have this level of curative activity upon single-dose oral administration (7).

## **Mutations in the P-type cation-transporter ATPase4 (PfATP4) confer low-level drug-resistance to spiroindolones**

The rapid development of drug resistance has plagued malaria control programs in almost all endemic regions. *In vitro* selection of resistance has proven to be a powerful predictor of the molecular determinants employed by parasites in field settings (21,22). To evaluate the potential for drug resistance and gain insight into the mechanism of action (MOA), we applied drug pressure to a cultured clone of Dd2—a multidrug-resistant parasite strain believed to have a higher propensity to mutate (23) (Fig. S3A). Six independent cultures were exposed to incrementally increasing sub-lethal concentrations of two compounds—NITD609 and the less potent derivative NITD678 (Fig. S3B and C). Following 3–4 months of constant drug pressure, the  $IC_{50}$  values had increased 7–24 fold (attaining a mean of 3–11 nM) for NITD609-selected parasites, and 7–11 fold (mean of 162–241 nM) for NITD678-selected parasites (Fig. S3D and E; Table S9). The relatively high number of passages required to yield drug-resistant parasites, together with the low level of resistance that was achieved, suggest that spiroindolones are not readily prone to select for high-level resistance *in vitro*. Subsequent passaging of drug-selected parasites in drug-free media for four months

showed no evidence of revertants, providing evidence that resistance was stable (Fig. S4). None of the selected mutants showed cross-resistance to a panel of antimalarial agents with diverse modes of action, including artemisinin and mefloquine (Table S10).

To determine the molecular basis of *in vitro* resistance, we prepared genomic DNA (gDNA) from each of the six drug-resistant clones. gDNA samples were then fragmented, labeled and hybridized to a high-density tiling array that contains ~6 million single-stranded 25-mer probes complementary to the *P. falciparum* genome. We compared the hybridization data for each haploid clone, using software that identifies regions on the array that show a loss or gain of hybridization relative to the non-resistant parental reference line (24), and that calculates a probability of a genomic change based on the number of consecutive probes showing a hybridization difference. The microarray covers approximately 90% of coding regions and 60% of non-coding regions, with probes spaced every 2 to 3 bases. Sequence coverage is limited only by the high AT content of *P. falciparum* that causes some 25-mer sequences to be represented more than once throughout the genome, rendering those non-informative (25). Former studies showed that this genome-tiling analysis can identify 90% of the differences that distinguish two strains in unique regions of the genome (24). Detectable genomic changes include single nucleotide polymorphisms (SNPs), insertion/deletion events and copy number variations (CNVs). Using a permissive p-value cutoff of  $1 \times 10^{-5}$ , we identified 7–95 genomic differences, localized to within 2–3 nucleotides, in each resistant clone. A similar comparison between two highly diverged strains such as Dd2 and 3D7 would yield >13,000 genomic differences (24). Using a stricter cutoff ( $p < 10^{-10}$ ) that should give fewer false positives at the expense of more false negatives, we found 27 total differences amongst all six mutants. Seven of these mapped to a single gene, *pfatp4* (PFL0590c; Fig. 3A and 3C), with the remainder found largely in randomly assorted subtelomeric or intergenic regions. Inspection of the hybridization patterns showed that one strain carried a copy number variant that encompassed the *pfatp4* locus (Fig. 3B). These data strongly suggest that treatment with spiroindolones specifically selects for mutations in *pfatp4*.

Sequencing of the entire *pfatp4* gene from the different resistant strains revealed eleven non-synonymous mutations (Table S9), with at least one in every clone. Nine of these were considered true genomic alterations for the thresholds used with the microarray analysis ( $p < 10^{-5}$ ). One exception resulted from a SNP lying within the copy number variant (NITD678-R<sup>Dd2</sup> clone#1). The second exception (NITD609-R<sup>Dd2</sup> clone#1) was the result of an emergent mixed population that had been cultured for several weeks after cloning in order to obtain enough DNA for hybridization. Sequencing of different PCR products from this clone showed that some fragments contained three mutations (Ile398Phe, Pro990Arg, and Asp1247Tyr) in *pfatp4* while others harbored only two mutations (Ile398Phe and Pro990Arg). The probability of 11 non-synonymous mutations occurring in *pfatp4* by chance is extremely unlikely. Sequencing of 14 different isolates of *P. falciparum* from different continents (26,27) revealed only 7 non-synonymous SNPs and 6 synonymous SNPs for *pfatp4* (from a total of ~32,000 SNPs), placing the gene at about the 70th percentile in terms of diversity. In contrast, none of the genes with the highest number of non-synonymous SNPs from sequencing field isolates (26,27) showed any differences in our tiling array analysis. Thus our data suggest a strong selective pressure on this single gene.

In order to confirm that drug resistance was conferred directly by these mutations, the full-length *pfatp4* gene was amplified from either wild-type or resistant lines, and cloned into an expression vector that allows for site-specific integration in transgenic parasites (Fig. S5). Following integrase-mediated recombination (28) to stably introduce these genes into parasites, transgenic lines were evaluated for inhibition of parasite growth as a function of drug concentration. Lines expressing mutant PfATP4 harboring either the single



Asp1247Tyr (D1247Y) or double Ile398Phe/Pro990Arg (I398F/P990R) mutations showed an increase in IC<sub>50</sub> values relative to the parental line (Fig. 4A and 4B; Table S11). This effect was enhanced when the I398F/P990R double mutant was placed under the control of the strong *P. falciparum* calmodulin (PF14\_0323) promoter, conferring a 5-fold increase in the IC<sub>50</sub> value against NITD609. The reduced level of resistance compared to the original drug-selected mutants can be attributed to the co-expression of variant *pfatp4* and the endogenous wild-type allele in our transfected lines. Artemisinin (Fig. 4C) and mefloquine (Fig. 4D) displayed equivalent potency against the wild-type and transgenic strains (Table S11), confirming that resistance was specific to the spiroindolones.

## Molecular characterization of PfATP4

The *pfatp4* gene product is annotated as a cation-transporting P-type ATPase (PfATP4) (29–31). This family of ATP-consuming transporters can be inhibited by chemically diverse compounds including thapsigargin, cyclopiazonic acid and lansoprazole, and as such constitutes an attractive set of drug targets (reviewed in (32)). P-type ATPases are ubiquitous in eukaryotic organisms and those involved in divalent cation transport appear to maintain a conserved structural mechanism for ion translocation (33). PfATP4 shows significant homology to *Saccharomyces cerevisiae* PMR1, a P-type ATPase required for high-affinity Ca<sup>2+</sup> and Mn<sup>2+</sup> transport. The human ortholog (hSPCA1) is associated with Hailey-Hailey disease, an acantholytic skin condition. The structural elucidation of a related rabbit SERCA pump (34), which shares 30% amino acid identity with PfATP4, enabled us to generate a homology model (Fig. 5). This localizes most of the eight resistance-associated mutations to transmembrane domains. The transmembrane region is predicted to act as a funnel to translocate cations across biological membranes, and includes eight conserved residues required for cation coordination (35,36). Importantly, none of those residues were altered in our resistant lines. We note that a number of P-type ATPase inhibitors, including cyclopiazonic acid and thapsigargin, bind to the transmembrane region (37–39). However, no cross-resistance to either inhibitor was observed in our spiroindolone-selected mutant parasite lines (Table S10).

To characterize PfATP4 further, we generated a PfATP4-GFP fusion that was co-transfected into Dd2 parasites along with mRFP-PfSec12, an endoplasmic reticulum (ER) marker (40). Live cell imaging of transgenic parasites localized PfATP4-GFP to the parasite plasma membrane throughout the intraerythrocytic lifecycle (Fig. 4E–F and Fig. S6). In late-stage segmented schizonts, this fusion protein was invaginated and surrounded the developing daughter merozoites, confirming a parasite plasma membrane distribution rather than delivery to the surrounding parasitophorous vacuole (Fig. 4F). This finding is supported by earlier immunofluorescence data that localized PfATP4 at or near the plasma membrane (30).

Several possibilities may explain how mutations in PfATP4 could confer resistance to spiroindolones. First, the protein could play a role in drug transport; however it shows no homology to known transporters. An alternative hypothesis could be that the PfATP4 mutations attenuate the spiroindolone-induced disruption of cellular homeostasis through an indirect mechanism that remains to be determined. Finally, PfATP4 may be the actual spiroindolones drug target since cation-transporting ATPases are chemically-validated drug targets (32). It is difficult to distinguish between these possibilities as little is known about the molecular function of PfATP4. We have been unable to reproduce results suggesting that PfATP4 plays a role in calcium transport (31) (Fig S7). And, it is unlikely that the protein regulates calcium transport of the endoplasmic reticulum calcium stores, given its localization to the plasma membrane. It is possible nonetheless that the protein regulates the trafficking of other cations. Although further functional characterization of PfATP4 is

clearly warranted, the mutations we identified will likely be useful molecular markers of drug resistance once NITD609 enters clinical trials.

## Conclusions

These studies define the spiroindolones as a new antimalarial chemotype that acts through a novel mechanism of action. In contrast to mefloquine and artemisinin, these compounds rapidly suppress protein synthesis in the parasite. Our genome-wide investigations revealed a specific mechanism of resistance mediated by the P-type ATPase PfATP4 and demonstrates at single-base resolution how a small eukaryotic genome adapts to sub-lethal drug pressure. Our lead compound NITD609 displays outstanding antimalarial activity, and meets all of the criteria required for a new antimalarial drug candidate. Further safety and pharmacological preclinical evaluation is currently ongoing to support the initiation of human clinical trials.

## Supplementary Material

Refer to Web version on PubMed Central for supplementary material.

## Acknowledgments

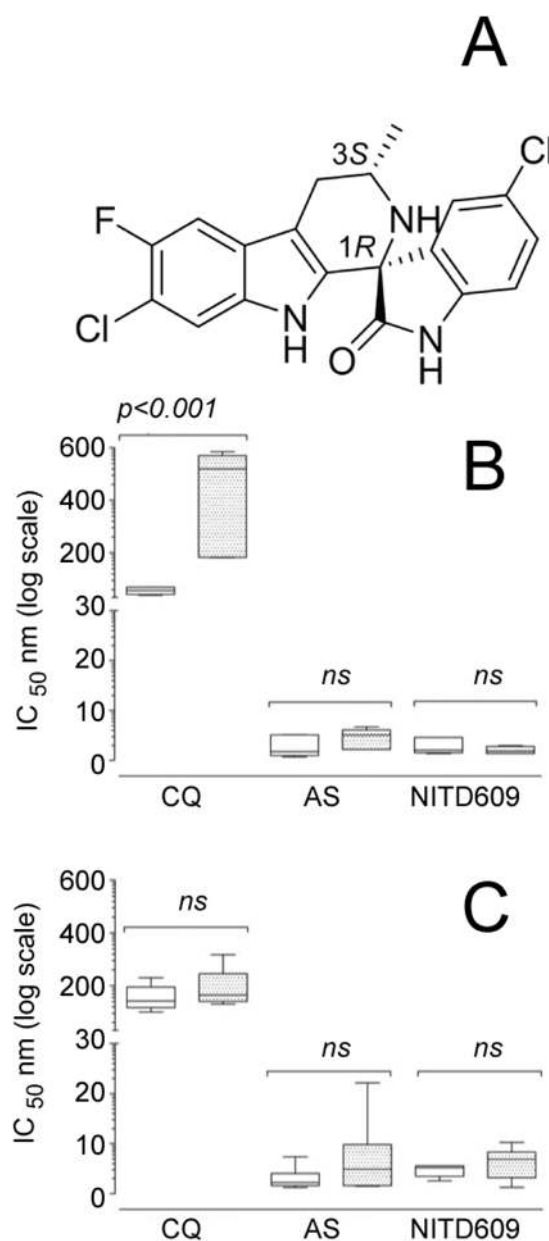
We thank Thomas A. Smith (SwissTPH) for the statistical analysis of the stage and rate of action studies. We thank Srinivasa Rao (NITD) and Martin Traebert (Novartis-preclinical safety) respectively for the cytotoxicity and hERG inhibition data. We also thank Margaret Weaver (Novartis-preclinical safety) for the interpretation of the preclinical toxicology data. The team would like to acknowledge Dr. Pete Schultz who had the vision to see the potential of these experiments in the exploratory phase. In addition, we extend our gratitude to Dr. Rich T. Eastman for providing guidance to help establish the in vitro drug selection protocol and for providing the cloned Dd2 parasites. Finally, the scientific expertise provided by Drs. Selina E.R. Bopp and Shailendra K. Sharma and their helpful discussions throughout this project were greatly appreciated. Funding for the PfATP4 transfectants was provided to the Fidock laboratory in part by the Medicines for Malaria Venture (MMV08/0015; PI D. Fidock). SMRU is sponsored by The Wellcome Trust of Great Britain, as part of the Oxford Tropical Medicine Research Programme of Wellcome Trust-Mahidol University. Laurent Renia laboratory is supported by a core grant from the Singapore Immunology Network, A\*STAR. This work was supported by a grant from the Medicines for Malaria Venture and a translational research grant (WT078285) from the Wellcome Trust to the Novartis Institute for Tropical Diseases, the Genomics Institute of the Novartis Research Foundation and the Swiss Tropical Institute and by grants to EAW from the W. M. Keck Foundation and NIH (R01AI059472).

## References

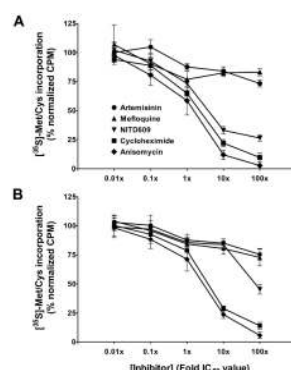
1. WHO. World Malaria Report. 2009. [http://www.who.int/malaria/world\\_malaria\\_report\\_2009/en/](http://www.who.int/malaria/world_malaria_report_2009/en/)
2. Greenwood BM, et al. J Clin Invest. 2008; 118:1266. [PubMed: 18382739]
3. Eastman RT, Fidock DA. Nat Rev Microbiol. 2009; 7:864. [PubMed: 19881520]
4. Dondorp AM, et al. N Engl J Med. 2009; 361:455. [PubMed: 19641202]
5. Noedl H, et al. N Engl J Med. 2008; 359:2619. [PubMed: 19064625]
6. White NJ. Science. 2008; 320:330. [PubMed: 18420924]
7. Olliaro P, Wells TN. Clin Pharmacol Ther. 2009; 85:584. [PubMed: 19404247]
8. Wells TNC, Alonso PL, Gutteridge WE. Nat Rev Drug Discov. 2009; 8:879. [PubMed: 19834482]
9. Winzeler EA. Nature. 2008; 455:751. [PubMed: 18843360]
10. Gamo FJ, et al. Nature. 465:305. [PubMed: 20485427]
11. Guiguemde WA, et al. Nature. 465:311. [PubMed: 20485428]
12. Plouffe D, et al. Proc Natl Acad Sci U S A. 2008; 105:9059. [PubMed: 18579783]
13. Russell BM, et al. Antimicrob Agents Chemother. 2003; 47:170. [PubMed: 12499187]
14. Guthmann JP, et al. Trop Med Int Health. 2008; 13:91. [PubMed: 18291007]
15. White NJ. J Antimicrob Chemother. 1992; 30:571. [PubMed: 1493976]
16. Sharrock WW, et al. Malar J. 2008; 7:94. [PubMed: 18505560]

17. Traebert M, Dumotier B. *Expert Opin Drug Saf.* 2005; 4:421. [PubMed: 15934850]
18. White NJ. *Lancet Infect Dis.* 2007; 7:549. [PubMed: 17646028]
19. Fidock DA, Rosenthal PJ, Croft SL, Brun R, Nwaka S. *Nat Rev Drug Discov.* 2004; 3:509. [PubMed: 15173840]
20. Vennerstrom JL, et al. *Nature.* 2004; 430:900. [PubMed: 15318224]
21. Hayton K, Su XZ. *Curr Genet.* 2008; 54:223. [PubMed: 18802698]
22. Nzila A, Mwai L. *J Antimicrob Chemother.* 2010; 65:390. [PubMed: 20022938]
23. Rathod PK, McErlean T, Lee PC. *Proc Natl Acad Sci U S A.* 1997; 94:9389. [PubMed: 9256492]
24. Dharia NV, et al. *Genome Biol.* 2009; 10:R21. [PubMed: 19216790]
25. Gardner MJ, et al. *Nature.* 2002; 419:498. [PubMed: 12368864]
26. Volkman SK, et al. *Nat Genet.* 2007; 39:113. [PubMed: 17159979]
27. Jeffares DC, et al. *Nat Genet.* 2007; 39:120. [PubMed: 17159978]
28. Nkrumah LJ, et al. *Nat Methods.* 2006; 3:615. [PubMed: 16862136]
29. Trottein F, Thompson J, Cowman AF. *Gene.* 1995; 158:133. [PubMed: 7789797]
30. Dyer M, Jackson M, McWhinney C, Zhao G, Mikkelsen R. *Mol Biochem Parasitol.* 1996; 78:1. [PubMed: 8813672]
31. Krishna S, et al. *J Biol Chem.* 2001; 276:10782. [PubMed: 11145964]
32. Yatime L, et al. *Biochim Biophys Acta.* 2009; 1787:207. [PubMed: 19388138]
33. Kuhlbrandt W. *Nat Rev Mol Cell Biol.* 2004; 5:282. [PubMed: 15071553]
34. Jensen AM, Sorensen TL, Olesen C, Moller JV, Nissen P. *EMBO J.* 2006; 25:2305. [PubMed: 16710301]
35. Clarke DM, Loo TW, Inesi G, MacLennan DH. *Nature.* 1989; 339:476. [PubMed: 2524669]
36. Toyoshima C, Nakasako M, Nomura H, Ogawa H. *Nature.* 2000; 405:647. [PubMed: 10864315]
37. Toyoshima C, Nomura H. *Nature.* 2002; 418:605. [PubMed: 12167852]
38. Moncoq K, Trieber CA, Young HS. *J Biol Chem.* 2007; 282:9748. [PubMed: 17259168]
39. Takahashi M, Kondou Y, Toyoshima C. *Proc Natl Acad Sci U S A.* 2007; 104:5800. [PubMed: 17389383]
40. Lee MC, Moura PA, Miller EA, Fidock DA. *Mol Microbiol.* 2008; 68:1535. [PubMed: 18410493]
41. Rice P, Longden I, Bleasby A. *Trends Genet.* 2000; 16:276. [PubMed: 10827456]

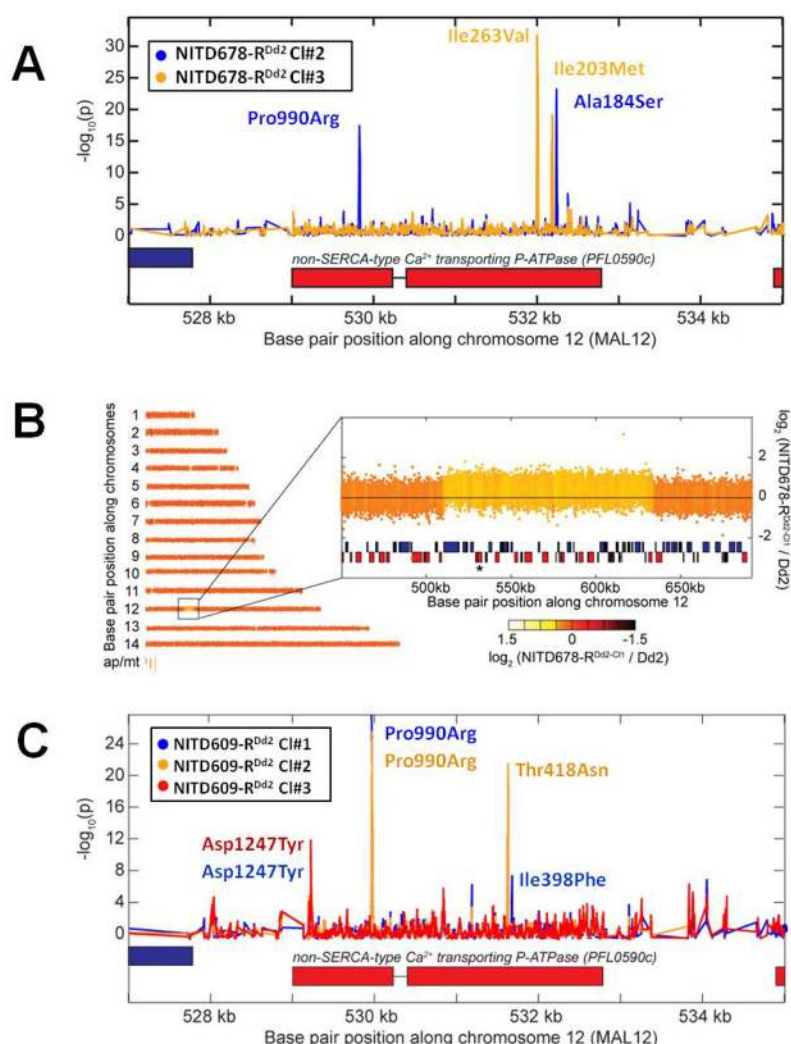


**Fig. 1.**

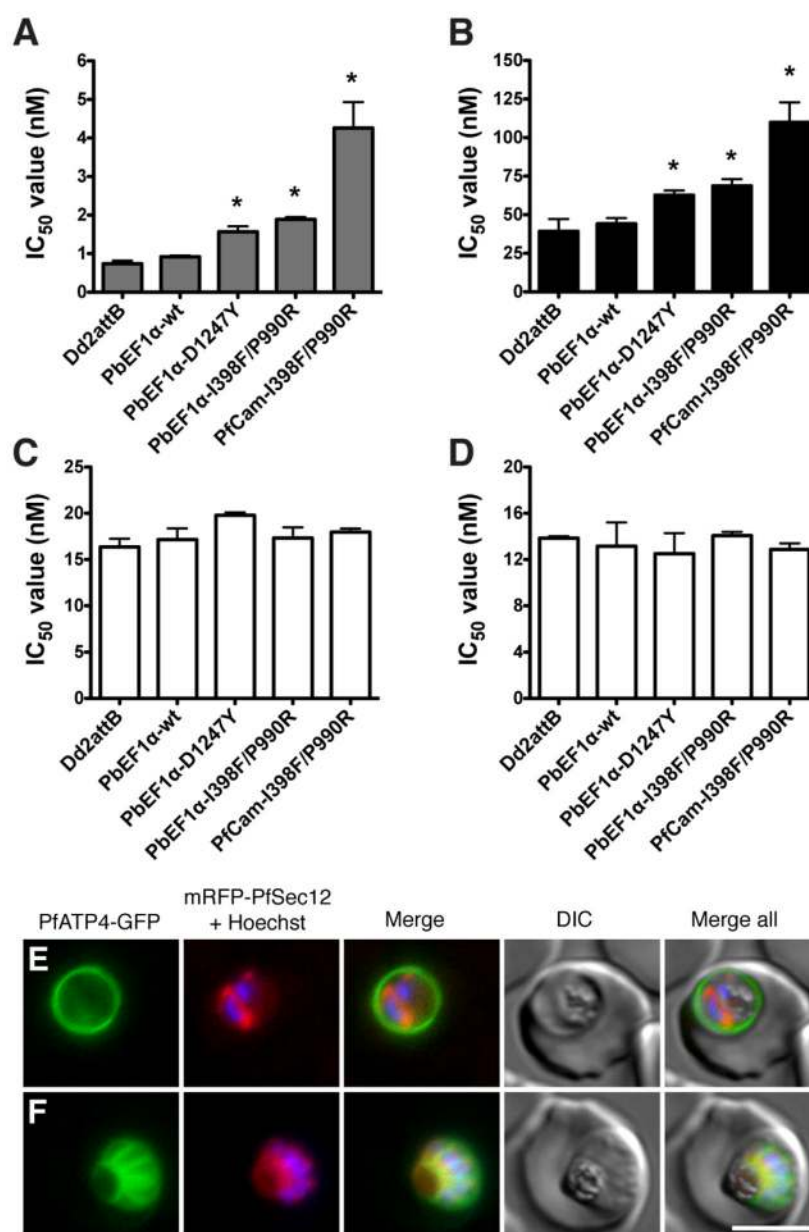
**(A)** Chemical structure of NITD609, showing the 1R,3S configuration that is essential for antimalarial activity. Key physicochemical properties are: solubility (pH 6.8) 39  $\mu\text{g/mL}$ ; logP (pH 7.4) 4.7; logD (pH 7.4) 4.6;  $pK_a^1$  4.7;  $pK_a^2$  10.7; polar surface area 56.92  $\text{\AA}^2$ . **(B)** *Ex vivo* sensitivity of *Plasmodium falciparum* and **(C)** *Plasmodium vivax* (9 and 10 clinical isolates respectively) to NITD609 compared with the reference drugs chloroquine and artesunate. The antimalarial sensitivity of these two species was measured after exposing ring (unshaded boxes) and trophozoite stages (shaded boxes) to drug for 20 h. Data are shown as max–min box plots, with the solid internal line indicating median  $IC_{50}$  values. Inhibition of parasite growth was determined after 42 hours. Only chloroquine-treated *P. vivax* displayed a significant stage-specific sensitivity ( $p < 0.001$ ).

**Fig. 2.**

Spiroindolones rapidly diminish protein synthesis in the parasite. The rate of parasite protein synthesis was evaluated by monitoring  $[^{35}\text{S}]$ -radiolabelled methionine and cysteine ( $[^{35}\text{S}]\text{-Met/Cys}$ ) incorporation into asynchronous cultures. Parasites were assayed for 1 hour in the presence of NITD609 (inverted triangle), anisomycin (diamond), cycloheximide (square), artemisinin (circle), or mefloquine (triangle), then extracted for radiographic measurements. Radiolabel incorporation was measured against inhibitor dosed over a five-log concentration range and percent incorporation was calculated by comparison to cultures assayed in the absence of inhibitor. Anisomycin and cycloheximide were included as positive controls. **(A)** Spiroindolone treatment rapidly diminishes protein synthesis in Dd2; however, this effect is mostly absent in **(B)** NITD609- $\text{R}^{\text{Dd2}}$  clone #2 except at very high concentration. 50% inhibition of  $[^{35}\text{S}]\text{-Met/Cys}$  incorporation was observed with **3x** and **78x**  $\text{IC}_{50}$  of NITD609 on the NITD609-treated Dd2 wild type and NITD609- $\text{R}^{\text{Dd2}}$  drug-resistant clones respectively. Data are expressed in mean $\pm$ SD and represent three independent experiments performed in triplicate. Similar losses of protein synthesis inhibition upon NITD609 treatment were observed in the resistant clones NITD609- $\text{R}^{\text{Dd2}}$  #1 and #3 respectively (see Fig. S2).

**Fig. 3.**

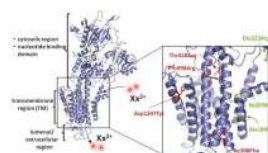
Genomic tiling arrays identified shared mutations in the *pfatp4* gene (PFL0590c) in all drug-resistant parasites. **(A)** Distinct pairs of single nucleotide polymorphisms (SNPs) in *pfatp4* were detected in NITD678-R<sup>Dd2</sup> clones #2 (blue) and #3 (orange). P-values were calculated for all probes covering *pfatp4* and flanking regions; a spike in the p-value reflects a difference in hybridization between the parental clone and the drug-selected clone, a hallmark of a SNP. Direct sequencing of *pfatp4* from each clone confirmed that these SNPs cause non-synonymous changes in the coding region, indicated by the red boxes. The resulting change in the primary sequence is given next to each SNP. **(B)** A 120kb copy number variation covering 37 genes in chromosome 12 was detected in the genome of NITD678-R<sup>Dd2</sup> clone #1. The *pfatp4* gene (asterisk) was contained within this amplification. Direct sequencing of *pfatp4* from this clone identified an additional non-synonymous SNP at amino acid position 223 (G223R). This mutation was continuously observed throughout numerous sequencing reads of sub-cloned *pfatp4* PCR products of NITD678-R<sup>Dd2</sup> clone #1, suggesting that the mutation occurred before the amplification event and, thus, resides in all *pfatp4* gene copies in the genome. **(C)** The three NITD609-R<sup>Dd2</sup> clones showed no evidence of copy number variants; however, each clone contained non-synonymous SNPs in *pfatp4* (clone #1, blue; clone #2, orange; clone #3, red).



**Fig. 4.** Introduction of mutant *pfatp4* into Dd2<sup>attB</sup> parasites decreases susceptibility to spiroindolones. *pfatp4* transgenes harboring mutations identified in either NITD609-R<sup>Dd2</sup> clone #1 (I398F/P990R) or clone #3 (D1247Y) were individually introduced into the parental Dd2 background to evaluate the ability of the mutant protein to protect against spiroindolone activity. As a control, wild-type *pfatp4* was also introduced. Expression of *pfatp4* was regulated by either the *P. berghei* EF1α promoter (PbEF1α) or the stronger *P. falciparum* calmodulin promoter (PfCam). IC<sub>50</sub> values were determined for (A) NITD609, (B) NITD678, (C) artemisinin, and (D) mefloquine. IC<sub>50</sub> values are shown as means±stdev and were derived from three independent experiments performed in quadruplicate with the SYBR Green-based cell proliferation assay (12). Statistical significance was calculated using a two-tailed unpaired t test, comparing transgenic *pfatp4* lines to the Dd2<sup>attB</sup> parental line: \*p<0.0001. (E, F) Localization of PfATP4 to the parasite plasma membrane.

Transgenic parasites co-expressing PfATP4-GFP and an ER marker, mRFP-PfSec12 were labeled with Hoechst 33382 to visualize the nucleus. PfATP4-GFP was observed at the parasite plasma membrane in **(E)** early schizont (two nuclei) and **(F)** late-segmented schizont parasites. Bar = 5  $\mu$ m.



**Fig 5.**

Resistance-associated SNPs map to the predicted transmembrane region of PfATP4. A homology model of PfATP4 was generated in SWISS-MODEL based on the crystal structure of the rabbit SERCA pump. Amino acid alignment analysis by EMBOSS (41) revealed 30% identity and 48% similarity between these proteins. Residues corresponding to resistance-associated mutations are indicated in red for NITD609-R<sup>Dd2</sup> and in green for NITD678-R<sup>Dd2</sup>. These mutations mapped to the putative transmembrane helices. The sites of divalent cation entry and exit are indicated as Xx<sup>2+</sup>.

Table 1

*In vivo* efficacy data in the *P. berghei* rodent malaria model.

Compound	1 × 10 mg/kg oral			1 × 30 mg/kg oral			1 × 100 mg/kg oral		
	Activity (%)	Survival (%)	Activity (%)	Survival (days)	Cure (%)	Activity (%)	Survival (days)	Cure (%)	
NIT609*	99.6	13.3	99.6	24.1	50	99.2	30	100	
Artesunate#	70	7.3	89	7.2	--	97	6.7	--	
Artemether#	81	6.2	97	6.9	--	99	7.6	--	
Chloroquine#	99.6	8	99.7	8.7	--	>99.9	12	--	
Mefloquine#	95	15.2	98	18.2	--	89	28	--	

Survival of control animals: 6–7 days

Cure = no parasite present at day 30

\* 0.5% MCM/0.1% Solutol HS15 formulation (n=10 mice)

# 7% Tween/3% Ethanol formulation (n≥10 mice)